Communication in Physical Sciences, 2024, 12(1): 120-140

Nickel-doped Zeolite cluster as adsorbent material for the adsorption of biodiesel oxidation products: Approach from computational study

Runde Musa, Uzairu Muhammad Sada and Favour A. Nelson Received: 18 September 2024/Accepted: 19 November 2024/Published 24 November 2024
doi:https://dx.doi.org/10.4314/cps.v12i1.10

Abstract: *This study investigates the adsorption behaviour of various biodiesel oxidation products onto the surface of nickel-doped zeolite as an efficient adsorbent zeolite (Ni-clo) through adsorption studies, quantum theory of atoms in molecules (QTAIM) analysis, and sensor performance evaluations using density functional theory. Adsorption studies reveal strong interactions between the surface and the biodiesel products, with ketone compounds exhibiting the most negative adsorption energy, indicating strong attraction to the Ni-clo surface. QTAIM analysis further elucidates the nature of these interactions, showing moderate to strong covalent bond formations and structural stability across all systems. Sensor performance evaluations highlight the electrical conductivity, charge transfer mechanism, back donation, and the fraction of electron transfer, indicating the potential of the sensor device to detect and desorb the targeted adsorbate. The findings suggest that the complexes exhibit relatively high reactivity. Overall, this comprehensive investigation provides insights into the adsorption behaviour and sensor performance of organic compounds on a Ni-clo zeolite surface.*

Keywords: *Biodiesel; oxidation; zeolite; adsorption; DFT*

Runde Musa
Department of Chemistry, National Open University of Nigeria, Abuja, Nigeria
Email: rmusa@noun.edu.ng
Orcid id: 0000-0001-9312-0455

Uzairu Muhammad Sada
Department of Chemistry, National Open University of Nigeria, Abuja, Nigeria
Email: muzairu@noun.edu.ng

Favour A. Nelson
Department of Pure and Applied Chemistry, University of Calabar, Calabar, Nigeria
Email: azogorfavour@gmail.com

1.0 Introduction

Biodiesel has been used as a substitute for petrodiesel in the transportation sector (Konur, 2021). Its main constituent is fatty acid methyl esters which are usually obtained in a process involving the transesterification of fats (animals or plants) with simple alcohols having short chains with methanol being mostly due to its cheap cost (Belousov *et al*., 2021Boss *et al*., 2022). In many countries, the use of biodiesel has increased over the years while in other countries it remains at an infancy status (Das andGundimeda, 2022). Biodiesel possesses more advantages than petrodiesel due to its reduced emissions of exhaust, biodegradability, domestic origin, and inherent lubricity (Das and Rokhum, 2024; Boas *et al*., 2022). Despite the many advantages of biodiesel, some shortcomings in its use have been observed where it auto-oxidizes at low temperatures and exhibits low thermal stability (Nielson, 2020; Tarhenia, 2020). Increased soot formation from the decomposition of biodiesel occurs due to the presence of C=C double bonds in the unsaturated fatty acid methyl esters (FAMEs) (Wei and Wang, 2021). Low combustion and reduced efficiency power can be triggered when there is a high level of unsaturation in the FAME molecules which affects oxygen content as well (Jafarihaghighi *et al*., 2020). The utilization of many feedstocks for the production of biodiesel varies concerning the region and its climate condition (Sing *et al*., 2020). For example, Thailand utilizes coconut oil, soybean oil is commonly used in the United

States and Brazil and palm kernel oil is often used in Southeast Asia regions (Mar *et* al., 2022; Lafarga, 2021). The similar characteristics of biodiesel to fuel such as complete miscibility have aided in its rising exploitation economically and its most common proportions (B_{20} and B_5) are used without modifications in engines (Malode *et al*., 2022; Xia, 2021). Therefore, gaining insights into the interaction and molecular effect of biodiesel on surfaces is of great importance in the effective augmentation and prediction of the performances of various fuel systems (Lee *et al*., 2021). In the past years, major success in the chemical industry in reducing environmental impact can be attributed to various catalytic reactions that are utilized worldwide (Ravanchi and Sahebdelfar, 2021). Catalysts perform the role of accelerating reaction rates and still maintain their originality and are destroyed or unrecovered when undergoing some secondary processes (Di *et al*., 2021; Wang *et al*., 2023). However, catalyst varies ranging from chemical to solid-supported catalysts (Aktary *et al*., 2024). Solid supported catalyst holds the phenomenon where reactive species are scarfed or grafted on a support material, therefore, enabling their recoverability and reusability for various procedures (Macfarlane *et al*., 2022). For an efficient solid-supported catalyst, an excellent supporting system having dispersed active species is required (Sachdeva *et al*., 2022). This process of using a solid supporting catalyst in a system is known as heterogeneous catalysis which is a fast-rising area of science due to its good attributes of cost-effectiveness, high selectivity, and energy efficiency (Belousov *et al*., 2022; Chaudhary *et al*., 2024). One of the first applications of heterogeneous catalysts was in the industrial field where nickel was used in producing margarine through hydrogenation of fats and oils (Mamontova *et al., 2023; Toshray*, 2024) Due to the robustness of transition elements, it has gained attention from researchers especially nickel (Ni) and palladium (Pd). These elements are diversified and easily modified to fit various applications (Ren *et* al., 2021; Wickham and Giri, 2021). In recent times, Ni has been widely used due to its highly reactive nature, high nucleophilic behaviour, small size, less toxicity, and abundant nature, unlike the other elements (Claver *et al*., 2020). These characteristics position Ni to be a good base for the adsorption and transformation of organic molecules that can be utilized in biodiesel development. Furthermore, the properties of Ni can be used to heighten the behaviour of various surfaces (Prabakaran *et al*., 2023). Zeolites, (CLO) a porous framework has been modified in recent years due to its selective adsorption nature (Dehmani et al*.,* 2023*).* . The discovery of zeolite was in the 18th century by Axel Fredrik, a Swedish mineralogist, who shed light on its properties and since then Zeolite has been introduced into the agriculture field (Bahrani *et al*., 2021). Zeolite has been characterized to have a high surface area, with a high potential to exchange ions which is important for a catalytic process (Zhang *et al*., 2022). Electron migration allows for dehydration to be reversed. Its high acidity, and thermal stability endeared attention to it in the industrial and environmental applications (Quadri *et al*., 2022). . Any member of the hydrated alumino-silicate mineral family is known as zeolite and they are classified based on the elements that make the entire framework. Due to the porous nature and the interconnectivity of the zeolite cavities, it can undergo a strain of modifications and serve as a catalyst and strong adsorbent in diverse chemical processes (Chen *et* al., 2020; Mallet *et al*., 2024). According to Du *et al*., (2022) in their study on pore structure and oxidation activity of soot formation from biodiesel use. Their findings state that soot reactivity increased when the surface became larger and the porosity became higher. The high oxygen content and low iodine number participated in the reduction of PM emissions and the

oxidation of the soot formed was accelerated (Du *et al*., 2022). In the literature of Blank and team on the various species of lubricant additives and their adsorption properties, it was concluded that the reactivity of protic molecules correlates with their adsorption energies and carboxylic possessed greater adsorption energy than alcohol using a γ-alumina surface (Blank *et al*., 2020).In a work by Zhang et al.(2021) on the high performance of nanoparticles in the production of biodiesel. Fe_3O_4@SBA-15-NH_2-HPW surface showcased high efficiency in the transesterification of palm oil using methanol and a high reusability potential. Also, in a comprehensive study encompassing the immobilization of a biodiesel model (lipase) on metal-organic frameworks (MOFs) by Shomal *et al*., Hierarchical mesoporous (ZIF-8 and ZIF-67) exhibited high catalytic activity having a conversion rate of 90% while HKUST-1 had a stronger chemical adoption enabling it to possess an increasing degree of reusability (Shomal *et al*., 2022). In this present study, five models of biodiesel (organic molecules); alcohol, aldehyde, ketone, carboxylic acid, and aromatic compounds were grafted on the Ni-CLO surface model, respectively. For the modification of the CLO pure surface to improve its properties, a single doping was performed, where one Ga atom was replaced with Ni. The interacted surfaces with the respective organic molecules were further optimized at a calculation method of DFT/B3LYP-D3Bj/LanL2DZ. This research aims at understanding adsorption pathways and gaining insights into the modelling of surfaces for the improvement of biofuel surfaces, therefore, also providing data on possible production of more efficient biodiesel models. Employing the first principle density function theory (DFT), the system's adsorption energies, nature of the bond, and interaction were ascertained.

2.0 Computational details

For the conceptualization of this study, a member of these organic compounds; alcohol, aldehyde, ketone, carboxylic acid, and aromatics are adsorbed on the Ni-CLO surface. The adsorption process is investigated using the density functional theory (DFT) at the B3LYP-D3BJ/LanL2DZ method. Employing the Gaussian09W software and Gauss view 6.0.16, (Gaussian, 2022' Gauss view, 2023). The systems were, sketched, optimized, and studied at a functional of B3LYP and a basic set of LanL2DZ. The calculation method is known for its maximum accuracy in adsorption studies (Khanifira *et al*., 2020). Various mathematical expression was employed in the evaluation of the electronic properties, sensor mechanism, and adsorption energies of the systems. The equation shown below was used for the determination of the adsorption energy where $E_{Molecule}$, $E_{Surface}$, and $E_{Complex}$ represents the adsorbate, surface, and complex energies.

$$E_{ad} = E_{complex} - (E_{surface} + E_{molecule}) \quad (1)$$

Chemcraft software is utilized for the visualization of the HOMO and LUMO energies and the Multiwfn application was used for obtaining the variables of the quantum theory of atoms-in-molecules (QTAIM) (Chemcraft, 2020; Lu *et al*., 2012). In addition, the visuals of the Non-covalent interaction (NCI) analysis were carried out employing the visual molecular dynamics (VMD) application Humphrey *et al*., 1996).

3.0 Results and Discussion

3.1 Ni-atom Spin-multiplicity

Spin multiplicity is the total number of possible spin states for electrons in the outermost shell of a metal atom (Sararaz *et al*., 2024). The spin values consist of 'up' or 'down'. Each electron in the atom contributes to the total spin state and the spin multiplicity accounts for all the possible combinations of these spins (Mariam, 2001). The spin multiplicity is calculated using the formula:

$$(2S+1) \quad (2)$$

where S is the electron spin quantum number and it can be calculated using the formula [50]:

$$S = \left|\sum_{i=1}^{N} s_i\right| \quad (3)$$

For this study, the spin multiplicity of Nickel is been analyzed. Nickel is a transitional metal with atomic number 28 thus it has an electronic configuration of $[Ar]3d^8 4s^2$ (Galperin *et al*., 1970). Thus to calculate its spin multiplicity, we know that there are 8 electrons in the 3d orbital and each electron has a quantum spin of s=0.5. Applying equation 2 to find the total spin quantum number:

$$S = \left|\sum_{i=1}^{8} \frac{1}{2}\right| = \left|4 \times \frac{1}{2}\right| = 2$$

Then apply equation 1 to calculate spin multiplicity: $= 2 \times 2 + 1 = 5$

Therefore the spin multiplicity of nickel is 5 which indicates that there are 5 possible spin states for the valence electrons in nickel (Fujimori and Minami, 1984(. Now from **Table 1,** four possible spins are recorded: singlet, triplet, quintet, and septet spins. The relative energies range from 0 to 0.2 approximately. The lower the relative energies, the more stable the atom. From the data below, the triplet multiplicity possesses a relative energy of zero. This means that, at triplet spin multiplicity, the Ni atom is in its ground state indicating that the triplet state is energetically favoured over other spin states (Upton *et al*., 1978). The reactivity of Ni in terms of multiplicity will then fall in increasing order: triplet > quintet > singlet > septet. The triplet state can even affect the magnetic behaviour of the atom thus since unpaired electrons are present the Ni atom may experience paramagnetism making the system susceptible to alignment in an external magnetic field (Alonso, 2000). These spin multiplicities may also impact the catalytic activity and selectivity of these complexes by affecting the accessibility of different electronic states and reaction pathways**(**Vogiatzis *et* al., 2018).

3.2 Structural analysis

The structural analysis is carried out to understand the stability of the compounds in terms of their bond lengths(Bag *et al*., 2017). **Table 2** gives a piece of vivid information on the different bond lengths in the compounds. From the results, the surface Ni-clo is been analyzed first. One atom of nickel is been doped on the zeolite surface and forms single bonds with three oxygen atoms O_7, O_8, and O_9.

Table 1. Spin multiplicity of Ni in singlet, triplet, quintet, and septet states evaluated at the B3LYP-D3BJ/LanL2DZ method. Energies measured in atomic units (a.u)

Multiplicity	Total Energies (a.u.)	Relative Energies (eV)
Singlet	-958.281644	0.1300
Triplet	-958.412712	0.000
Quintet	-958.353003	0.059
Septet	-958.186239	0.226

The bond formed between Ni and O_8 is of more interest since it's the only bond that tends to distort when biodiesel product interacts with the surface. The Ni_{25}-O_8 has a bond length of 1.893A. Ga_{16}-H_{21}, Ga_{16}-O_{17}, and P_{12}-H_{24} bonds are also considered negligible for all the compounds as some of their magnitudes differ by just 0.001. For the interactions, the major bonds of interest occur between Ni and an atom from the biodiesel products. The biodiesel products include alcohols with OH functional, aldehydes with CO functional, aromatics with double bond/ rings as a symbol of their functionality, carboxylic acids with functional COOH and ketones with CO functional (Gundekari *et al*., 2020). ll these products tend to behave differently due to their functional groups since functional groups decide on the chemical behavior of compounds (Hrabic and Keefer, 2002). From the second column on Table 2, the bond length between Ni and the targeted functional groups is being observed. The alcohol interaction ALC-Ni-clo forms an interaction between Ni_{25} and O_{33} from its OH functional at a magnitude of 1.953A while the aldehyde forms the bond Ni_{25}-O_{31} with the

oxygen atom arising from it CO functional group at a magnitude of 1.926A. The aromatic compound which is typically benzene has a bond distance of 2.83A from Ni_{25} since it doesn't form any actual bond with the surface. The carboxylic acid compound forms the bond Ni_{25}-O_{31} from its COOH functional at a length of 1.974 while the ketone compound forms the bond Ni_{25}-O_{27} from its – functional at a length of 1.98A. From the interactions discussed above, we can see that the aldehydes form the smallest bond length with the surface followed by the alcohol group then the carboxylic acid group, ketone and lastly the aromatic group which happens to form the longest bond length with the surface. This means that the surface Ni-clo forms more stable interactions with the aldehydes and alcohols, moderately with the carboxylic and ketones and unstable with the aromatics.

Table 2. Bond lengths formed within the surface and interactions measured calculated at the B3LYP-D3BJ/LanL2DZ

Compound	Ni25-O8 (Å)	Ni25-Functional Group (Å)	Ga16-H21 (Å)	Ga16-O17 (Å)	P12-H24 (Å)
Ni-clo	1.893	--	1.554	1.808	1.432
ALC-Ni-clo	1.969	1.953	1.556	1.803	1.431
ALD-Ni-clo	1.914	1.926	1.556	1.804	1.431
ARO-Ni-clo	1.889	2.830	1.553	1.803	1.431
CAR-Ni-clo	1.958	1.974	1.556	1.802	1.431
KET-Ni-clo	1.977	1.980	1.556	1.804	1.431

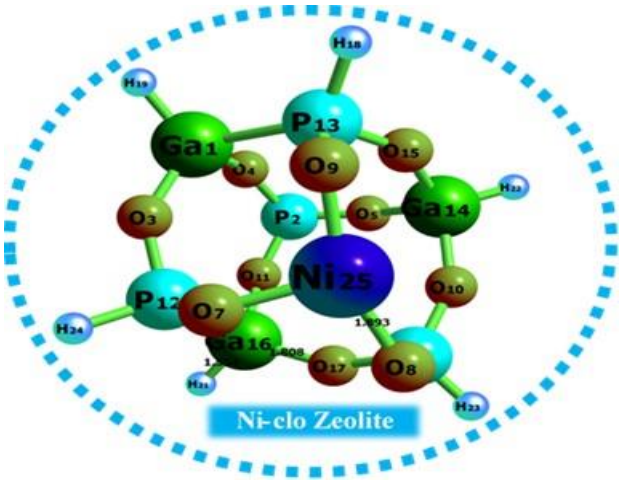

Fig. 1. Illustration of Ni-doped zeolite structure (Ni-clo)

3.3 Electronic properties

3.3.1 HOMO-LUMO analysis

Most literature reviews investigate the electronic properties of any studied compound, positioning the FMO (Frontier Molecular Orbital) study to be vital in understanding the intricacies surrounding the electronic properties of a system (Bakheit *et al*., 2023). The FMO has further been classified into two major regions. These regions signify the

position and flow of electrons from one state to another within a system which characterizes the electronic conductivity, therefore, affecting the nature of stability of that system (Dearnaley *et al*., 1970). The highest occupied molecular orbital (HOMO) region acts as a point where electron excitation is induced, propelling their transfer from one orbital to the other, and is often termed to be an electron donor (Maitra, 2017). In contrast to the HOMO, the lowest unoccupied Molecular Orbital (LUMO) is known as the electron-deficient region or vacant orbital, which readily accepts the donated electrons from the HOMO (Etabu *et al*., 2022' Zhan *et al*., 2003). Notably, the difference in the HOMO and LUMO regions termed the energy gap is a crucial parameter in quantifying the reactivity within a system. A range of equations **(a) – (e)** has been utilized in this study for the computation of Table 3 (Eddy *et al*., 2011)

Electronegativity (χ) $= \frac{IP+E.A}{2}$ (a)

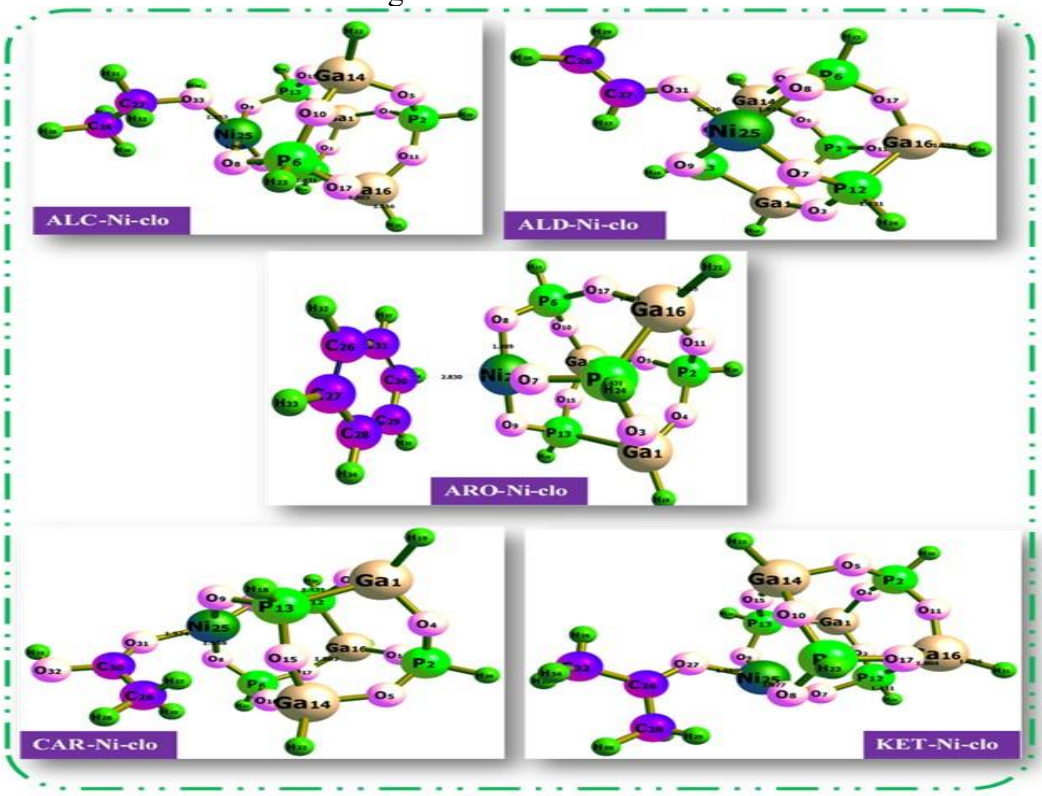

Figure 2. Structural illustration of interactions between biodiesel products and the Ni-clo surface

Chemical hardness (η) $= \frac{IP-E.A}{2}$ (b)

Electron donating power (ω^-) $= \frac{(u^-)2}{2\eta^-} \approx \frac{(3\,IP+E.A)^2}{16(IP-E.A)}$ (c)

Electrophilicity index (ω) $= \frac{u^2}{2 \times \eta}$ (d)

Electrochemical potential (μ) = $-\chi$ (e)

All FMO studied parameters are presented in Table 3. From Table 3**,** the energy gap values (E_g) fall within the range of 3.3 eV to 4.3 eV with a noticeable increase in the interactions. These gap values evaluate the reactivity, and stability of the modeled system concerning the trends observed across the systems (Eemia and Shahidehpour, 2013). Here, the Ni-CLO surface exhibited a low energy gap value of 3.560 eV as compared to its interacted counterparts, positioning it to be slightly reactive with and high stability level. Within the complexes, the ARO-Ni-CLO complexes possessed the lowest energy gap value of 3.382

eV while ALD-Ni-CLO complex holds the highest energy gap values which infer ARO-Ni-CLO to be least reactive with increased stability while ALD-Ni-CLO is the most reactive complex and the least stable which agrees with existing literature on the subject. Correlatively, the observation in the electronegativity values shed light on an electron potential to attract electron positions (Cherkasov *et al*., 1998). ARO-Ni-CLO possesses the highest electron-attracting ability due to its large electronegative value. The high electrophilicity index values of the complexes suggest them to be strong electrophiles (Chartaraj and Roy, 2007). and Ni-CLO surfaces to exhibit a better adsorption rate for the studied five organic compounds. Furthermore, a minimal decrease in the chemical hardness values of the complexes as compared to the pure surface (Ni-CLO) depicts a slight increase in the reactivity of the system upon adsorption (Gber *et al*., 2023). The pictorial representation of electron transfer from one region to another within the systems is presented in Fig. 3**,** this explicitly collates element contribution by the evaluation of element behaviours. Iso surfaces representing charge transfers are observed in Fig. 3.

3.3.2 NBO analysis

In Chemistry, an in-depth understanding of a compound's stability can be achieved by the effective utilization of the Natural Bond Orbital analysis. This analysis explicitly describes and evaluates electron movement and molecular stability (Zhang *et al*., 2020). The second-order perturbation energy which describes and categorizes various chemical interactions present in a system is a very important parameter here (Gonzalez-Diaz *et al*., 2013). In this study, NBO analysis is employed to decipher the delocalization of electrons in the studied organic compounds on the Ni-CLO bare surface. It aids the observation of the intermolecular interaction between and within the donor and acceptor regions of an orbital which measures the stabilization energy and establishes the strength of interactions existing in the molecules (Saral *et al*., 2024).

Table 3. Frontier Molecular Orbital (FMO) parameters for compounds evaluated at the B3LYP-D3BJ/LanL2DZ

System	E_{HOMO} (eV)	E_{LUMO} (eV)	Egap (eV)	IP (eV)	EA (eV)	μ	η	S	ω	EFL (eV)
Ni-clo	-6.999	-3.438	3.560	6.999	3.438	5.219	1.780	0.281	7.649	-5.219
ALC-Ni-clo	-6.812	-2.761	4.051	6.812	2.761	4.786	2.025	0.247	5.655	-4.786
ALD-Ni-clo	-6.819	-2.537	4.281	6.819	2.537	4.678	2.141	0.234	5.112	-4.678
ARO-Ni-clo	-6.770	-3.388	3.382	6.770	3.388	5.079	1.691	0.296	7.628	-5.079
CAR-Ni-clo	-6.770	-2.889	3.881	6.770	2.889	4.829	1.940	0.258	6.009	-4.829
KET-Ni-clo	-6.713	-2.770	3.943	6.713	2.770	4.742	1.972	0.254	5.701	-4.742

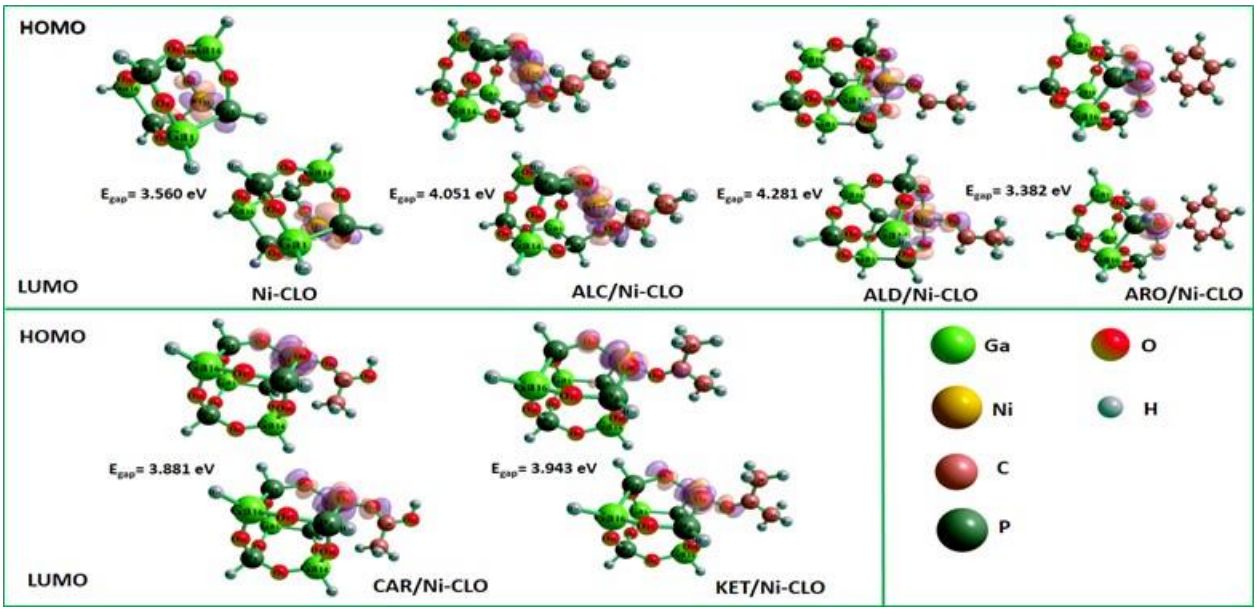

Fig. 3. Pictorial representation of the transfer of electrons between HOMO and LUMO in the interactions.

In Table 4, the NBO calculations are presented as bonding and anti-bonding orbital for the donor and acceptor of the lone pair, the stabilization energy, and the Fock matrix. From Table X, the surface, Ni-CLO, possesses a high E^2 value of 608.76 kcal/mol, positioning it to be stable and least reactive. These characteristics reflect how stable and readily modified this surface can be. However, a trend of increased reactivity was observed upon the interaction with the organic compounds, alcohol, aldehyde, carboxylic acid, aromatics, and ketone respectively. Amongst the interactions, ALC-Ni-CLO was the least stable because it possesses a small E^2 value of 158.71 kcal/mol as compared to its counterparts complexes while KET-Ni-CLO reflects a higher stability level and the least reactivity and conductivity among the studied complexes at a donor orbital of σ* P_6 - O_{10} and acceptor region of LP*(1) Ga_{14} and this depicts the occurrence of a stronger interaction.

Table 4. Natural Bond Order (NBO) analysis data for interactions evaluated at the B3LYP-D3BJ/LanL2DZ

System	Donor	Acceptor	E^2 (kcal/mol)	E(i)-E(j)	F(i,j)
Ni-clo	σ O8 - Ni25	σ* O7 - Ni25	608.76	0.02	0.212
ALC-Ni-clo	LP*(1) Ga1	σ* O3 - P12	158.71	0.02	0.113
ALD-Ni-clo	LP*(1) Ga1	σ* O3 - P12	148.87	0.02	0.114
ARO-Ni-clo	BD*(2) C29 - C30	BD*(2) C27 - C28	198.89	0.02	0.084
CAR-Ni-clo	π* O9 - Ni25	σ* O8 - Ni25	124.46	0.01	0.097
KET-Ni-clo	σ* P6 - O10	LP*(1) Ga14	259.84	0.01	0.099

3.3.3 d-band center

The d-band is the center position of the PDOS equivalent to d-orbitals (Fuggle *et al*., 1983). The d-band center of transitional metals is a fundamental factor used in elucidating and predicting the modifications in chemisorption strength of tiny molecules on transition metal structures and it is meticulously linked with the

action of surface catalysis in these systems (Montemore *et al*., 2017). Normally the position of the d-band is relative to the Fermi level (E_{FL}), thus a positive d-band center indicates that the average energy level of the d-orbital lies above the Fermi level while negative d-band centers have average energies of the d-orbitals lying below the Fermi level (Adachi, 1997). Also, positive d-band centers are linked with weak binding of adsorbates to the surface (Xin *et al*., 2014). In catalysis, positive d-band centers propose that the surface is less likely to adsorb and activate reactant molecules, and metals with positive d-band centers are typically less reactive towards adsorbates and may exhibit lower catalytic activity for certain reactions, therefore, the lower the value of the d-band, the stronger the adsorption of these smaller molecules on the transitional metal (Bhattacharjee *et al*., 2016). With all this information being laid down, the d-band for the surfaces below is being calculated. From **Table 5** below, the center of Total Density of States (TDOS) is tabulated in the first column and falls between the ranges of -9.2eV to approximately -9.7eV. The center of the Partial Density of States (PDOS) is also calculated based on the number of transitional metals present and in this study, only Nickel is present. The surface Ni-clo has a center of PDOS of -4.99eV. ALC-Ni-clo has a PDOS center of -4.96eV, ALD-Ni-clo has a PDOS center of -5.06eV, ARO-Ni-clo with -4.77eV, CAR-Ni-clo with -4.94eV and KET-Ni-clo with -4.90eV. The d-band center is calculated using the formula:

d-band center = center of PDOS - Fermi level corresponding to HOMO level (4)

From the results acquired using this formula, the d-band center for all the compounds is positive which suggests generally weak adsorption of the small systems by these metals. This is called physisorption **[76]**. Although the values of the d-band center are positive they fall within the ranges of 1.1 eV and 1.5 eV approximately. Since these values lie closer to zero, there's a slight possibility of experiencing little chemisorption between the Ni atom and other small molecules. From Table 5, the d-band center of the surface Ni-clo is calculated to be 1.18 eV. After interaction with the different biodiesel products, the value of the d-band center increases for all the compounds. The alcohol group increases the d-band center to a value of 1.41 eV, the aldehydes to a value of 1.32 eV, the aromatics to 1.44eV, the carboxylic group to a value of 1.38 eV, and the ketones to a value of 1.49 eV. The order of decrease in d-band value is given as Ketones > Aromatics > Alcohols > carboxylic > Aldehydes > Ni-clo. This means that the aldehydes are more attracted to the Ni atom in terms of adsorption than the ketones.

3.4 Adsorption studies

Adsorption studies are carried out to understand the interaction between the adsorbate and the adsorbent (Aguayo-Vilencia and Gonzalez *et al*., 2020). . Adsorption energy is the energy required for the adsorbate and adsorbent to interact with each other. The more negative the adsorption energy, the stronger the interaction (Qu *et al*., 2018). This means that negative adsorption energies indicate chemisorption in the systems (Kralik, 2014). From Table 6, the energies of the surface Ni-clo and the interactions are recorded in hartrees while the adsorption energy is converted to electron volts (eV). The ketone biodiesel products show the most negative adsorption energy among the compounds having a magnitude of about -7.1eV which means that the ketone compounds are greatly attracted to the Ni-clo zeolite surface. This is followed by the alcohol and aldehyde biodiesel products which possess an adsorption energy of -3.5eV. The carboxylic group trails behind with an adsorption energy of -3.3eV and lastly the aromatics with the highest adsorption energy of -2.7eV. The increasing order of attraction for the biodiesel products to the Ni-clo surface is given as ARO > CAR > ALC=ALD > KET.

Table 5. Values of Total Density of States (TDOS), Partial Density of State (PDOS) and d-band of surface Ni-clo and interactions evaluated at the B3LYP-D3BJ/LanL2DZ

Compound	Center of TDOS (eV)	Center of PDOS (eV)	Fermi Level (HOMO Level) (eV)	d-band Center (eV)
Ni-clo	-9.28	-4.99	-6.17	1.18
ALC-Ni-clo	-9.66	-4.96	-6.38	1.41
ALD-Ni-clo	-9.72	-5.06	-6.37	1.32
ARO-Ni-clo	-9.77	-4.77	-6.21	1.44
CAR-Ni-clo	-9.72	-4.94	-6.32	1.38
KET-Ni-clo	-9.73	-4.90	-6.39	1.49

The adsorption studies give general information on how the entire adsorbent is being adsorbed on the adsorbate. Unlike the d-band studies, it gives a complete outlook on the behaviour of interacted molecules on the surface. This is why the ketone group may show strong adsorption in general but physical adsorption concerning the transitional metal in the d-band analysis.

3.5 Quantum Theory of Atoms in Molecules (QTAIM)

The quantum theory of atoms in molecules (QTAIM) is a topological analysis carried out to understand the interactions occurring in a compound in terms of its electron density, energy density, electron localization function (ELF), and the Laplacian of electron density alongside other parameters (Poater *et al*., 2005). From Table 7 all data related to QTAIM are recorded. The bond critical points (BCPs) indicate that chemical bonds are present in the compound (Pakiari and Eskandari, 2006).

Table 6. The adsorption energy of the interactions with Ni-clo evaluated at the B3LYP-D3BJ/LanL2DZ

Compounds	$E_{adsorbate(Ni-clo)}$= -958.28 hartrees		
	$E_{complex}$ (Hartrees)	$E_{adsorbent}$ (Hartrees)	E_{ads}(eV)
ALC-Ni-clo	-1113.45	-155.04	-3.537
ALD-Ni-clo	-1112.23	-153.82	-3.537
ARO-Ni-clo	-1190.62	-232.24	-2.721
CAR-Ni-clo	-1187.47	-229.07	-3.265
KET-Ni-clo	-1151.56	-193.02	-7.075

Interactions between the surface and the biodiesel products are of utmost concern. Beginning with the alcohol biodiesel products, the first interaction Ni_{25}-O_{33} has an electron density of 0.71a.u and a Laplacian of 0.56a.u. The energy density (H(r)) and the potential energy density (V(r)) are both negative which implies that a strong interaction is established between the alcohol group and the zeolite (Nakanish *et al*., 2008). This particular interaction proves the strong reactivity of the Nickel atom which tells us that the system might relatively be in its singlet or septet spin multiplicity. The ELF is at 0.54a.u which confirms the strength of the bond. Its second eigenvalue (λ_2) is negative thus the interaction is composed of attractive forces and the interaction is structurally stable due to low ellipticity. The second interaction Ga_{16}-P_{12} has an electron density of 0.48a.u and a Laplacian

of 0.68a.u. The V(r) and H(r) give a strong covalent interaction and have an ELF of 0.92a.u showing extreme localization of the bond. λ_2 is positive thus steric repulsion is prevalent in the bond at a magnitude of 0.15a.u. Its ellipticity is much lower thus it is structurally more stable than the first interaction. In the aldehyde biodiesel products, Ni_{25}-O_{31} interaction is observed to have an electron density of 0.94a.u and a Laplacian of 0.96a.u. The V(r) and H(r) relationship indicates a moderate interaction since only V(r) is negative. Strong localization is shown with an ELF of 0.90a.u. λ_2 shows steric hindrance and the ellipticity is very low (negative value: -2.65a.u) indicating high structural stability. The second interaction O_9-H_{32} has a very low electron density of 0.16a.u and Laplacian of 0.81, V(r) H(r) relationship shows moderate interaction with ELF of 0.32 a.u indicating delocalized bonds, a negative λ_2, and ellipticity of 0.5a.u. For the aromatic compound, the interaction Ni_{25}-C_{30} is observed to have low values of electron density and Laplacian of the electron density. The H(r) V(r) relationship shows a strong covalent interaction with an ELF of 0.15a.u showing strong delocalization of the bond. A negative λ_2 is observed with an ellipticity of 0.3a.u. The second interaction is very similar to the second interaction observed in the alcohol. The carboxylic compound forms two major interactions, Ni_{25}-O_{31} and Ni_{25}-H_{28} with electron densities of 0.66a.u and 0.73a.u respectively and Laplacian of approximately 0.5a.u for both interactions. The magnitude of their ELF is approximately 0.5a.u and 0.63a.u respectively. The first interaction is dominated by attractive forces while the second experiences steric repulsion. The two interactions prove that the system might be slightly structurally unstable due to relatively high ellipticity (Gagner *et al*., 2018). In the ketone interaction, the Ni_{25}-O_{27} has an electron density of 0.65a.u with a Laplacian of 0.53a.u. The H(r) V(r) relationship denotes a strong covalent interaction and an ELF of 0.47a.u is observed which represents a slightly delocalized bond. There's a presence of attractive forces and the system observes structural stability relatively. The last interaction Ni_{25}-C_{26} has very low electron density and Laplacian as well. The bond shows a moderate interaction with ELF of 0.43a.u experiencing forces of attraction and achieving structural stability. In summary, the interactions within all the systems either show moderate or strong covalent bond formation, more localized bonds than the delocalized ones and relative structural stability.

3.6 Sensor performances

One core area in developing a sensor device is the device's ability to sense the targeted adsorbate and further, the potential of an adsorbed material to be desorbed for the sustainability of the device. Here, various interrelated parameters such as the electrical conductivity, charge transfer mechanism, and back donation, are utilized in investigating the potential of the sensor device and solidifying the reports from other studied analyses in the literature (Yon *et al*., 2018).

Work function and Charge transfer mechanism

The energy values of the HOMO and LUMO presented in the electronic studies are employed in analyzing the charge transfer mechanism ratio of studied systems. Observing the work function values, ranged from 4.60 to 5.1 eV which suggests the systems have a good adsorbing quality since high work function values indicate a better sensing potential (Zhang *et al*.,2022). The charge transfer focuses on the electron movement and flow through different states which directly affects the conductivity, reactivity, and stability of a particular system and this is possible by the evaluation of the distribution of the electron density within the molecules (Barbara *et al*., 1996).

According to existing works of literature, values of the quantum descriptor follow trends

Table 7. Quantum Theory of Atoms in Molecules (QTAIM) analysis data. The units of all parameters are given as follows: P(r), e/Ang^3; ∇^2 ρ(r), e/Ang^3; λ_1, λ_2, and λ_3 have a unit of e/Ang^5 respectively; G(r) and V(r) have units of eV; H(r) has a unit of eVAng^3/e; ellipticity of electron density (ε), electron localization function (ELF) and λ_1/ λ_3 are dimensionless. The unit of G/|V| is Ang^3.

System	Interaction	BCPs	P(r)	$\nabla^2\rho(r)$	G(r)	V(r)	H(r)	Gr/Vr	ELF	LOL	λ_2	λ_3	ε
ALC-Ni-clo	Ni25-O33	53	0.71	0.56	0.15	-0.15	-0.59	-1.00	0.54	0.19	-0.45	-0.61	0.35
	Ga16-P12	74	0.48	0.68	0.65	-0.18	-0.11	-3.61	0.92	0.68	0.15	-0.42	0.06
ALD-Ni-clo	Ni25-O31	53	0.94	0.96	0.21	-0.17	0.36	-1.24	0.90	0.15	0.10	-0.15	-2.65
	O9-H32	126	0.16	0.81	0.17	-0.13	0.35	-1.31	0.32	0.15	-0.12	-0.18	0.50
ARO-Ni-clo	Ni25-C30	56	0.22	0.26	0.11	-0.16	-0.50	-0.69	0.15	0.30	-0.13	-0.16	0.30
	Ga16-P12	63	0.47	0.67	0.65	-0.17	-0.11	-3.82	0.92	0.67	0.15	-0.41	0.29
CAR-Ni-clo	Ni25-O31	155	0.66	0.53	0.13	-0.14	-0.22	-0.93	0.52	0.19	-0.38	-0.88	1.33
	Ni25-H28	161	0.73	0.54	0.14	-0.15	-0.70	-0.93	0.63	0.21	0.68	-0.89	0.67
KET-Ni-clo	Ni25-O27	231	0.65	0.53	0.14	-0.14	-0.26	-1.00	0.47	0.18	-0.28	-0.47	0.65
	Ni25-C26	108	0.20	0.11	0.24	-0.21	0.35	-1.14	0.43	0.15	-0.18	0.56	-1.32

where lower values depict that a shorter distance is required for charges to be transferred and larger values posit that a longer distance is needed for molecules to interact within a system and charges to be likely transferred (May and Kuhn, 2023). These trends affect the system's nature and control a range of compound behaviour. Thus, the charge transfer mechanism was studied using equation 5

$$Qt = Q_{adsorption} - Q_{isolated} \quad (5)$$

Where Qt represents the charge transfer and $Q_{adsorption}$ and $Q_{isolated}$ connotes the transfer of charge in molecules pre and post-adsorption. It has been observed and recorded in other research works that a positive charge transfer value denotes the movement of charges from a material to the adsorbate and it characterizes the good sensing behaviour of a system while the negative value suggests the flow of charges from the adsorbate to the material. Due to the organic compounds investigated and the sensor nature, the Bader charge theory is utilized. The charge transfer values for the respective studied compound are presented in Table 8**.** The adsorption values are minimal and the Q_t values for all systems are negative which describes an average potential to be used in the sensing of the studied organic compound respectively. In **Table 8**, ARO-Ni-CLO complex possessed the highest Q_t value of -0.715 eV, implying a substantial transfer of charge between the adsorbate and the adsorbent material. Similar to ARO-Ni-CLO, CAR-Ni-CLO complex had a value of -0.957 eV and ALC-Ni-CLO complex possessed the lowest Q_t value of -1.641 eV and this suggests that it has a lower degree of transferring charges from the adsorbate and the adsorbent material. Therefore, the sensing potential is in ascending order of ALC-Ni-CLO, KET-Ni-CLO, ALD-Ni-CLO, CAR-Ni-CLO, ARO-Ni-CLO, and ARO-Ni-CLO complex is suggested to be more reactive than its studied counterparts.

Electrical conductivity

Insights into the behaviors of a material under the influence of an electric field are gained through the understanding of the electrical conductivity of the materials. This parameter encompasses the current flow from the adsorbent material to the adsorbed gas or adsorbate and can be deduced from the energy gap values of the quantum descriptors (Tabari and Farmanzadeh, 2020). . The electrical conductivity is calculated using the mathematical expression shown in equation 6. The equation for the electrical conductivity (σ) is comprised of a constant temperature (T), Energy gap (E_g), and Boltzmann constant (K), respectively.

$$\sigma = AT^{2/3}e^{(E_g/2KT)} \quad (6)$$

With evidence from previous literature, the electrical conductivity can be evaluated by the trends in the energy gap, where a decrease in the energy gap leads to an increase in the electrical conductivity (Amat *et al*., 2014). Therefore, according to Table 8 and equation 6, ARO-Ni-CLO complex possesses the highest conducting potential as compared to the other complexes while ALD-Ni-CLO complex indicates the lowest conductivity.

Fraction of electron transfer (FET) and back donation

The back donation (ΔE) exemplifies the transfer of an electron from the adsorbate to the adsorbent materials and the concurrent interaction between the surface and the gas which describes the strength of adsorption that occurs between molecules (Cazorla 2015). Consequently, the nature and location of the charge transfer from the adsorbate to the adsorbent is directly influenced and examined by the fraction of electron transfer (ΔN) which are presented in Table 8. The ΔE and ΔN values are calculated employing the mathematical expression below.

$$\Delta E_{Back\ donation} = -\frac{\eta}{4} \quad (7)$$

$$\Delta N = \frac{\chi_{isolated} - \chi_{system}}{2\,(\eta_{isolated} - \eta_{system})} \quad (8)$$

It has been stated in literature that chemical hardness values greater than zero and negative ΔE values substantiate a material to have good sensing potential (Tajee *et al*., 2024). The fraction of electron transfer (FET) is confirmed by the range of the chemical hardness values, where a negative correlation is usually observed in the values. Low chemical hardness values of a system significantly showcase the high FET of that system and this indicates a great flow of electron transfer upon the interaction of the adsorbate and adsorbent (Raimi *et al.* 2024). Therefore, in this study, the back donation values for all systems are all negative, implying the presence of a stronger adsorption process between the adsorbent and the studied organic compounds respectively. Also, the chemical hardness values connote a slight variation in the stability of the systems since the values are in the range of 1.6 eV to 2.2 eV and stronger adsorption. Ni-CLO surface showcased a heightened potential for adsorbing aromatic compounds as compared to other studied organic compounds.

Table 8. Sensor mechanism parameters for interactions (Note: The unit of ϕ is in eV, Qt in electron (e) and that of ΔN is dimensionless.

System	Eads (eV)	ϕ/eV	Qt (e)	ΔE Back-donation	ΔN
ALC-Ni-CLO	-3.693	4.786	-1.641	-0.506	-0.884
ALD-Ni-CLO	-3.511	4.678	-1.394	-0.535	-0.749
ARO-Ni-CLO	-2.685	5.079	-0.715	-0.423	0.787
CAR-Ni-CLO	-3.321	4.829	-0.957	-0.485	-1.219
KET-Ni-CLO	-3.704	4.742	-1.448	-0.493	-1.242

4.0 Conclusions

In conclusion, this study delves into the intricate interactions between the biodegradation products of biodiesel and nickel-doped zeolite material, shedding light on their adsorption behavior and sensor performance. Through adsorption studies and QTAIM analysis, we discerned the strong affinity of ketone compounds towards the Ni-clo surface, indicating potential applications in biodiesel production. Sensor performance evaluations underscored the importance of electrical conductivity, charge transfer mechanism, and back donation in assessing the sensing potential of the adsorbent material. Overall, this research contributes to the understanding of molecular interactions on surfaces and advances the development of sensor devices for environmental monitoring and industrial applications.

5.0 References

Adachi, H. (1997). Molecular cluster approach to electronic state and chemical bonding in metallic materials. *Materials Transactions, JIM*, *38*, 6, pp. 485–502.

Aguayo-Villarreal, I. A., Cortes-Arriagada, D., Rojas-Mayorga, C. K., Pineda-Urbina, K., Muñiz-Valencia, R., & Gonzalez, J. (2020). Importance of the interaction adsorbent–adsorbate in the dyes adsorption process and DFT modeling. *Journal of Molecular Structure, 1203*, , pp. 127398.

Aktary, M., Alghamdi, H. S., Ajeebi, A. M., AlZahrani, A. S., Sanhoob, M. A., Aziz, M. A., & Nasiruzzaman Shaikh, M. (2024). Hydrogenation of CO2 into Value-added Chemicals Using Solid-Supported Catalysts. *Chemistry–An Asian Journal*, e202301007.

Alonso, J. A. (2000). Electronic and atomic structure, and magnetism of transition-metal clusters. *Chemical Reviews*, 100, 2, pp. 637–678.

Amat, A., Mosconi, E., Ronca, E., Quarti, C., Umari, P., Nazeeruddin, M. K., ... & De Angelis, F. (2014). Cation-induced band-gap tuning in organohalide perovskites: interplay of spin–orbit coupling and octahedra tilting. *Nano Letters, 14*, 6, pp. 3608–3616.

Bag, P., Porzelt, A., Altmann, P. J., & Inoue, S. (2017). A stable neutral compound with an aluminum–aluminum double bond. *Journal of the American Chemical Society*, 139, 41, pp. 14384–14387.

Bahrani, S., Ghaedi, M., Tariq, R., Zalipour, Z., & Sadeghfar, F. (2021). Fundamental developments in the zeolite process. In *Interface Science and Technology*, 32, pp. 499–556.

Bakheit, A. H., Abuelizz, H. A., & Al-Salahi, R. (2023). Hirshfeld Surface Analysis and Density Functional Theory Calculations of 2-Benzyloxy-1, 2, 4-triazolo [1, 5-a] quinazolin-5 (4 H)-one: A Comprehensive Study on Crystal Structure, Intermolecular Interactions, and Electronic Properties. *Crystals, 13*, 10, doi.org/10.3390/cryst13101410

Barbara, P. F., Meyer, T. J., & Ratner, M. A. (1996). Contemporary issues in electron transfer research. *The Journal of Physical Chemistry, 100*, 31, pp. 13148–13168.

Belousov, A. S., Esipovich, A. L., Kanakov, E. A., & Otopkova, K. V. (2021). Recent advances in sustainable production and catalytic transformations of fatty acid methyl esters. *Sustainable Energy & Fuels, 5, 18, pp.* 4512–4545.

Belousov, A. S., Esipovich, A. L., Kanakov, E. A., & Otopkova, K. V. (2021). Recent advances in sustainable production and catalytic transformations of fatty acid methyl esters. *Sustainable Energy & Fuels*, 5, 18, pp. 4512–4545.

Bhattacharjee, S., Waghmare, U. V., & Lee, S. C. (2016). An improved d-band model of the catalytic activity of magnetic transition metal surfaces. *Scientific Reports, 6*, 1, pp. 35916.

Blanck, S., Loehlé, S., Steinmann, S. N., & Michel, C. (2020). Adhesion of lubricant on aluminium through adsorption of additive head-groups on γ-alumina: A DFT study. *Tribology International*, 145, pp. 106140. DOI:10.1016/j.triboint. 2019.106140

Blanck, S., Loehlé, S., Steinmann, S. N., & Michel, C. (2020). Adhesion of lubricant on aluminium through adsorption of additive head-groups on γ-alumina: A DFT study. *Tribology International*, 145, DOI:10.1016/j.triboint.2019.106140.

Cazorla, C. (2015). The role of density functional theory methods in the prediction of nanostructured gas-adsorbent materials. *Coordination Chemistry Reviews, 300*, , pp. 142–163.

Chattaraj, P. K., & Roy, D. R. (2007). Update 1 of: Electrophilicity index. *Chemical Reviews, 107*, 9, pp. PR46–PR74.

Chaudhary, R. G., Potbhare, A. K., Aziz, S. T., Ayyub, M. M., Kahate, A., Madankar, R. S., ... & Mahmoud, S. H. (2024). Bioinspired Graphene-based Metal Oxide Nanocomposites for Photocatalytic and Electrochemical Performances: An Updated Review. *Nanoscale Advances.*DOI:10.1039/D3NA01071F

Chen, L. H., Sun, M. H., Wang, Z., Yang, W., Xie, Z., & Su, B. L. (2020). Hierarchically structured zeolites: from design to application. *Chemical Reviews*, 120, 20, pp. 11194–11294.

Cherkasov, A. R., Galkin, V. I., Zueva, E. M., & Rafael'A, C. (1998). The concept of electronegativity. The current state of the problem. *Russian Chemical Reviews, 67*, 5, pp. 375–392.

Claver, C., Yeamin, M. B., Reguero, M., & Masdeu-Bultó, A. M. (2020). Recent advances in the use of catalysts based on natural products for the conversion of

CO_2 into cyclic carbonates. *Green Chemistry*, 22, 22, pp. 7665–7706.

Das, A., & Rokhum, S. L. (2024). *Renewable diesel and biodiesel: A comparative analysis. In Renewable Diesel* (pp. 123–166). Elsevier.

Das, P., & Gundimeda, H. (2022). Is biofuel expansion in developing countries reasonable? A review of empirical evidence of food and land use impacts. *Journal of Cleaner Production, 372*, 133501. https://doi.org/10.1016/j.jclepro.-2022.133501.

Dearnaley, G., Morgan, D. V., & Stoneham, A. M. (1970). A model for filament growth and switching in amorphous oxide films. *Journal of Non-Crystalline Solids, 4*, pp. 593–612.

Dehmani, Y., Mohammed, B. B., Oukhrib, R., Dehbi, A., Lamhasni, T., Brahmi, Y., ... & Abouarnadasse, S. (2023). Adsorption of various inorganic and organic pollutants by natural and synthetic zeolites: A critical review. *Arabian Journal of Chemistry*, 105474. doi.org/10.1016/j.arabjc.2023.105474.

Di, L., Zhang, J., Zhang, X., Wang, H., Li, H., Li, Y., & Bu, D. (2021). Cold plasma treatment of catalytic materials: A review. *Journal of Physics D: Applied Physics, 54(33),* DOI: 10.1088/1361-6463/ac0269

Du, J., Su, L., Zhang, D., Jia, C., & Yuan, Y. (2022). Experimental investigation into the pore structure and oxidation activity of biodiesel soot. *Fuel*, 310, pp. 122316. DOI: 10.1016/j.fuel.2021.122316.

Eddy, N. O. and Ita, B. I. (2011). Experimental and theoretical studies on the inhibition potentials of some derivatives of cyclopenta-1,3-diene. *International Journal of Quantum Chemistry* 111(14): 3456-3473. DOI:10.1002/qua

Eremia, M., & Shahidehpour, M. (Eds.). (2013). *Handbook of electrical power system dynamics: Modeling, stability, and control*. John Wiley & Sons.

Etabti, H., Fitri, A., Benjelloun, A. T., Benzakour, M., & Mcharfi, M. (2022). Efficient tuning of benzocarbazole based small donor molecules with D-π-A-π-D configuration for high-efficiency solar cells via π-bridge manipulation: A DFT/TD-DFT study. *Computational and Theoretical Chemistry, 1208*, , pp. 113580.

Fayemi, O. E., & Ebenso, E. E. (2022). Functionalized carbon allotropes as corrosion inhibitors. In *Functionalized nanomaterials for corrosion mitigation: Synthesis, characterization, and applications* (pp. 87–114). American Chemical Society.

Fuggle, J. C., Hillebrecht, F. U., Zeller, R., Zołnierek, Z., Bennett, P. A., & Freiburg, C. (1983). Electronic structure of Ni and Pd alloys. I. X-ray photoelectron spectroscopy of the valence bands. *Physical Review B, 27*, 4, doi.org/10.1103/PhysRevB.27.2179

Fujimori, A., & Minami, F. (1984). Valence-band photoemission and optical absorption in nickel compounds. America *Physical Society*, 30(2), doi:10.1103/PhysRevB.30.957.

Gagner, J. E., Qian, X., Lopez, M. M., Dordick, J. S., & Siegel, R. W. (2012). Effect of gold nanoparticle structure on the conformation and function of adsorbed proteins. *Biomaterials, 33*, 33, pp. 8503–8516.

Galperin, F. M., & Gavrilov, N. A. (1970). The Electronic Structure of 3d Transition Metals. *Physica Status Solidi (b)*, 40(1), pp. 53–58.

Gaussian 16, Revision C.01, M. J. Frisch, G. W. Trucks, H. B. Schlegel, G. E. Scuseria, M. A. Robb, J. R. Cheeseman, G. Scalmani, V. Barone, G. A. Petersson, H. Nakatsuji, X. Li, M. Caricato, A. V. Marenich, J. Bloino, B. G. Janesko, R. Gomperts, B. Mennucci, H. P. Hratchian, J. V. Ortiz, A. F. Izmaylov, J.

L. Sonnenberg, D. Williams-Young, F. Ding, F. Lipparini, F. Egidi, J. Goings, B. Peng, A. Petrone, T. Henderson, D. Ranasinghe, V. G. Zakrzewski, J. Gao, N. Rega, G. Zheng, W. Liang, M. Hada, M. Ehara, K. Toyota, R. Fukuda, J. Hasegawa, M. Ishida, T. Nakajima, Y. GaussView, Version 6.1, Roy Dennington, Todd A. Keith, and John M. Millam, Semichem Inc., Shawnee Mission, KS, 2016.

Khnifiraa, M., El Hamidia, S., Machrouhia, A., Mahsounea, A., Boumyaa, W., Tounsadia, H., ... & Abdennouria, M. (2020). Theoretical and experimental study of the adsorption characteristics of Methylene Blue on titanium dioxide surface using DFT and Monte Carlo dynamic simulation. *Homo*, 2(2).

Chemcraft - graphical software for visualization of quantum chemistry computations. Version 1.8, build 682. https://www.chemcraftprog.com.

Gber, T. E., Louis, H., Ngana, O. C., Amodu, I. O., Ekereke, E. E., Benjamin, I., ... & Adeyinka, A. (2023). Yttrium-and zirconium-decorated $Mg_{12}O_{12}$–X (X= Y, Zr) nanoclusters as sensors for diazomethane (CH_2N_2) gas. *RSC Advances*, *13*, 36, pp. 25391–25407.

Gonzalez-Diaz, H., Arrasate, S., Gomez-SanJuan, A., Sotomayor, N., Lete, E., Besada-Porto, L., & M Ruso, J. (2013). General theory for multiple input-output perturbations in complex molecular systems. 1. Linear QSPR electronegativity models in physical, organic, and medicinal chemistry. *Current Topics in Medicinal Chemistry*, *13*, 14, pp. 1713–1741.

Gundekari, S., Mitra, J., & Varkolu, M. (2020). Classification, characterization, and properties of edible and non-edible biomass feedstocks. In *Advanced Functional Solid Catalysts for Biomass Valorization* (pp. 89–120). Elsevier.

Hrabie, J. A., & Keefer, L. K. (2002). Chemistry of the nitric oxide-releasing diazeniumdiolate ("nitrosohydroxylamine") functional group and its oxygen-substituted derivatives. *Chemical Reviews*, 102, 4, pp. 1135–1154.

Humphrey, W., Dalke, A., & Schulten, K. (1996). "VMD - Visual Molecular Dynamics," *J. Molec. Graphics*, 14, pp. 33–38.

Jafarihaghighi, F., Ardjmand, M., Salar Hassani, M., Mirzajanzadeh, M., & Bahrami, H. (2020). Effect of fatty acid profiles and molecular structures of nine new sources of biodiesel on combustion and emission. *ACS Omega, 5, 26, pp.* 16053–16063.

Konur, O. (2021). Biodiesel and petrodiesel fuels: Science, technology, health, and the environment. In *Biodiesel Fuels* (pp. 3–36). CRC Press.

Králik, M. (2014). Adsorption, chemisorption, and catalysis. *Chemical Papers*, *68*, 12, pp. 1625–1638.

Lafarga, T. (2021). Production and consumption of oils and oilseeds. In *Oil and Oilseed Processing: Opportunities and Challenges* (pp. 1–21).

Lee, C. C., Tran, M. V., Tan, B. T., Scribano, G., & Chong, C. T. (2021). A comprehensive review on the effects of additives on fundamental combustion characteristics and pollutant formation of biodiesel and ethanol. *Fuel*, *288*, pp. 119749.

MacFarlane, L., Zhao, C., Cai, J., Qiu, H., & Manners, I. (2021). Emerging applications for living crystallization-driven self-assembly. *Chemical Science*, 12, 13, pp. 4661–4682.

Maitra, N. T. (2017). Charge transfer in time-dependent density functional theory.

Journal of Physics: Condensed Matter, 29, 42, DOI 10.1088/1361-648X/aa836e

Mallette, A. J., Shilpa, K., & Rimer, J. D. (2024). The Current Understanding of Mechanistic Pathways in Zeolite Crystallization. *Chemical Reviews. Chem. Rev.* 124, pp. 3416-3493 DOI: 10.1021/acs.chemrev.3c00801.

Malode, S. J., Gaddi, S. A. M., Kamble, P. J., Nalwad, A. A., Muddapur, U. M., & Shetti, N. P. (2022). Recent evolutionary trends in the production of biofuels. *Materials Science for Energy Technologies, 5*, pp. 262–277.

Mamontova, E., Trabbia, C., Favier, I., Serrano-Maldonado, A., Ledeuil, J. B., Madec, L., ... & Pla, D. (2023). Novel Catalyst Composites of Ni-and Co-Based Nanoparticles Supported on Inorganic Oxides for Fatty Acid Hydrogenations. *Nanomaterials*, 13, 9, pp. 1435.

Marian, C. M. (2001). Spin-orbit coupling in molecules. *Reviews in Computational Chemistry*, 17, pp. 99–204.

May, V., & Kühn, O. (2023). *Charge and energy transfer dynamics in molecular systems*. John Wiley & Sons.

Montemore, M. M., Van Spronsen, M. A., Madix, R. J., & Friend, C. M. (2017). O_2 activation by metal surfaces: Implications for bonding and reactivity on heterogeneous catalysts. *Chemical Reviews, 118*, 5, pp. 2816–2862.

Mulliken, R. S. (1932). The interpretation of band spectra part III. Electron quantum numbers and states of molecules and their atoms. *Reviews of Modern Physics,* 4, 1, pp. 1.

Nakanishi, W., Hayashi, S., & Narahara, K. (2008). Atoms-in-molecules dual parameter analysis of weak to strong interactions: behaviors of electronic energy densities versus Laplacian of electron densities at bond critical points. *The Journal of Physical Chemistry A, 112*, 51, pp. 13593–13599.

Nielsen, C. F. (2020). *Discovery and characterization of formate dehydrogenases for enzymatic conversion of CO2*.

Pakiari, A. H., & Eskandari, K. (2006). The chemical nature of very strong hydrogen bonds in some categories of compounds. *Journal of Molecular Structure: THEOCHEM, 759*, 1–3, pp. 51–60.

Pal, P., Ting, J. M., Agarwal, S., Ichikawa, T., & Jain, A. (2021). The catalytic role of D-block elements and their compounds for improving sorption kinetics of hydride materials: a review. *Reactions, 2*, 3, pp. 333–364.

Poater, J., Duran, M., Sola, M., & Silvi, B. (2005). Theoretical evaluation of electron delocalization in aromatic molecules by means of atoms in molecules (AIM) and electron localization function (ELF) topological approaches. *Chemical Reviews, 105*, 10, pp. 3911–3947.

Prabakaran, S., Rupesh, K. J., Keeriti, I. S., Sudalai, S., Venkatamani, G. P., & Arumugam, A. (2023). A scientometric analysis and recent advances of emerging chitosan-based biomaterials as potential catalyst for biodiesel production: A review. *Carbohydrate Polymers*, 121567.doi.org/10.1016/j.carbpol.2023.121567

Qu, Z., Sun, F., Liu, X., Gao, J., Qie, Z., & Zhao, G. (2018). The effect of nitrogen-containing functional groups on SO_2 adsorption on carbon surface: Enhanced physical adsorption interactions. *Surface Science, 677*, , pp. 78–82.

Raimi, M. A., Rajee, A. O., Gber, T. E., Arikpo, T. O., Pembere, A., & Louis, H. (2024). Cobalt group transition metals (TM: Co, Rh, Ir) coordination of S-doped porphyrins (TM_S@ PPR) as sensors for molecular SO_2 gas adsorption: a DFT and QTAIM study. *Journal of Molecular Modeling, 30*, 3, pp. 1–18.

Rajee, A. O., Amodu, I. O., Abdlateef, M. K., Ogbogu, M. N., Ibrahim, R. H., Adesope, K. T., ... & Louis, H. (2024). Chemically effect of small molecules (X= CF_3, COOH, NH_2, NO_2) functionalized covalent organic framework (X-COF) as sensors for glyphosate: A computational study. *Chemical Physics Impact*, , , pp. 100510.

Ravanchi, M. T., & Sahebdelfar, S. (2021). Catalytic conversions of CO2 to help mitigate climate change: Recent process developments. *Process Safety and Environmental Protection*, *145*, pp. 172–194.

Ren, X., Han, Y., Xu, Y., Liu, T., Cui, M., Xia, L., Li H., Gu Y., Wang, P. (2021). Diversified strategies based on nanoscale metal-organic frameworks for cancer therapy: The leap from monofunctional to versatile. *Coordination Chemistry Reviews*, 431, pp. 213676. doi.org/10.1016/j.ccr.2020.213676

Sachdeva, G., Vaya, D., Rawat, V., & Rawat, P. (2022). *Solid-supported Catalyst in Heterogeneous Catalysis. In Heterogeneous Catalysis in Organic Transformations* (pp. 105–125). CRC Press.

Saral, A., Manikandan, A., Javed, S., & Muthu, S. (2024). Vibrational spectra, molecular level solvent interaction, stabilization, donor-acceptor energies, thermodynamic, non-covalent interaction and electronic behaviors of 6-Methoxyisoquinoline-anti tubercular agent. *Chemical Physics Impact, 8*, , pp. 100392.

Sarfaraz, S., Yar, M., & Ayub, K. (2024). The electronic properties, stability and catalytic activity of metallofullerene (M@C60) for robust hydrogen evolution reaction: DFT insights. *International Journal of Hydrogen Energy*, 51, pp. 206–221.

Shomal, R., Du, W., & Al-Zuhair, S. (2022). Immobilization of Lipase on Metal-Organic frameworks for biodiesel production. *Journal of Environmental Chemical Engineering*, 10, 2, doi.org/10.1016/j.jece.2022.107265

Singh, D., Sharma, D., Soni, S. L., Sharma, S., Sharma, P. K., & Jhalani, A. (2020). A review on feedstocks, production processes, and yield for different generations of biodiesel. *Fuel,* doi.org/10.2516/ogst/2020088

Tabari, L., & Farmanzadeh, D. (2020). Yttrium doped graphene oxide as a new adsorbent for H_2O, CO, and ethylene molecules: Dispersion-corrected DFT calculations. *Applied Surface Science, 500*, , pp. 144029.

Tahernia, M. (2020). *Papertronic sensing arrays for rapid and high-throughput screening of electroactive microorganisms* (Doctoral dissertation). State University of New York at Binghamton.

Tian Lu, Feiwu Chen, Multiwfn: A Multifunctional Wavefunction Analyzer, *J. Comput. Chem.* 33, pp. 580–592, DOI: 10.1002/jcc.22885.

Toshtay, K. (2024). Liquid-phase hydrogenation of sunflower oil over platinum and nickel catalysts: Effects on activity and stereoselectivity. *Results in Engineering*, 101970. doi.org/10.1016/j.rineng.2024.101970

Upton, T. H., & Goddard III, W. A. (1978). The electronic states of Ni2 and Ni2+. *Journal of the American Chemical Society*, 100, 8, pp. 5659–5668.

Vilas Bôas, R. N., & Mendes, M. F. (2022). A review of biodiesel production from non-edible raw materials using the transesterification process with a focus on the influence of feedstock composition and free fatty acids. *Journal of the Chilean Chemical Society, 67, 1, pp.* 5433–5444.

Vilas Bôas, R. N., & Mendes, M. F. (2022). A review of biodiesel production from non-edible raw materials using the transesterification process with a focus on the influence of feedstock composition and free fatty acids. *Journal of the Chilean Chemical Society*, 67, 1, pp. 5433–5444.

Vogiatzis, K. D., Polynski, M. V., Kirkland, J. K., Townsend, J., Hashemi, A., Liu, C., & Pidko, E. A. (2018). Computational approach to molecular catalysis by 3d transition metals: challenges and opportunities. *Chemical Reviews*, 119, 4, pp. 2453–2523.

Wang, A., Du, M., Ni, J., Liu, D., Pan, Y., Liang, X., ... & Wang, W. (2023). Enhanced and synergistic catalytic activation by photoexcitation-driven S− scheme heterojunction hydrogel interface electric field. *Nature Communications*, *14*, *1*, *pp.* 6733. https://doi.org/10.1038/341467-023-42542-6.

Wei, J., & Wang, Y. (2021). Effects of biodiesels on the physicochemical properties and oxidative reactivity of diesel particulates: A review. *Science of The Total Environment*, *788*, 147753. https://doi.org/10.1016/j.scitotenv.2021.147753.

Wickham, L. M., & Giri, R. (2021). Transition metal (Ni, Cu, Pd)-catalyzed alkene dicarbofunctionalization reactions. *Accounts of Chemical Research*, 54, 17, pp. 3415–3437.

Xia, S. (2021). Production, application, and future development of biodiesel. Thesis submitted to Centria University of Applied Science, Finland. https://urn.fi/URN:NBN:fi:amk-2021092217967

Xin, H., Vojvodic, A., Voss, J., Nørskov, J. K., & Abild-Pedersen, F. (2014). Effects of d-band shape on the surface reactivity of transition-metal alloys. *Physical Review B*, *89*, 11, DOI: 10.1103/PhysRevB.89.115114

Yoon, J., Yang, H. S., Lee, B. S., & Yu, W. R. (2018). Recent progress in coaxial electrospinning: New parameters, various structures, and wide applications. *Advanced Materials*, *30*, 42, pp. 1704765.

Zhan, C. G., Nichols, J. A., & Dixon, D. A. (2003). Ionization potential, electron affinity, electronegativity, hardness, and electron excitation energy: molecular properties from density functional theory orbital energies. *The Journal of Physical Chemistry A*, *107*, 20, pp. 4184–4195.

Zhang, J. X., Sheong, F. K., & Lin, Z. (2020). Principal interacting orbital: A chemically intuitive method for deciphering bonding interaction. *Wiley Interdisciplinary Reviews: Computational Molecular Science*, *10*, 6, pp. e1469.

Zhang, L., Li, Z., Yang, J., Zhou, J., Zhang, Y., Zhang, H., & Li, Y. (2022). A fully integrated flexible tunable chemical sensor based on gold-modified indium selenide nanosheets. *ACS Sensors*, *7*, 4, pp. 1183–1193.

Zhang, P., Liu, P., Fan, M., Jiang, P., & Haryono, A. (2021). High-performance magnetite nanoparticles catalyst for biodiesel production: Immobilization of 12-tungstophosphoric acid on SBA-15 works effectively. *Renewable Energy*, 175, pp. 244–252.

Zhang, Q., Gao, S., & Yu, J. (2022). Metal sites in zeolites: synthesis, characterization, and catalysis. *Chemical Reviews*, 123, 9, pp. 6039–6106. Quadri, T. W., Olasunkanmi, L. O.,

Elendu, C. C., Wang, Z., Aleem, R. D., Cao, C., Duan, P. G., Ramzan, N., & Hazzan, O. O. (2024). Environmental impact and performance evaluation of calabash seed oil biodiesel. *Biomass and Bioenergy*, *183*, 107152. https://doi.org/10.1016/j.biombioe.2023.107152

Acknowledgments

The authors would like to acknowledge the TetFund Institutional Base Research and the Management of the National Open University of Nigeria for their financial support during conducting this research. We also acknowledge the Centre for High Performance Computing (CHPC), South Africa for providing some computational resources for this research project.

Declaration
Compliance with Ethical Standards
Declaration
Ethical Approval

Not Applicable

Competing interests

The authors declare that they have no known competing financial interests.

Funding

The work was funded by TETfund under IBR

Availability of data and materials

Data would be made available on request.

Authors' Contribution

Runde Musa: Conceptualization, supervision and writing. Uzairu Muhammad Sada: Formal analysis, writing and reviewing. Favour A. Nelson: writing of first draft, revision and editing.